ACS OMEGA

Open Access

http://pubs.acs.org/journal/acsodf

Article

Unveiling the Innate and Adaptive Immunity Interplay: Global Transcriptomic Profiling of the Host Immune Response in *Candida albicans* Endophthalmitis in a Murine Model

Agimanailiu Khapuinamai, Dhanwini Rudraprasad, Suchita Pandey, Dilip Kumar Mishra, and Joveeta Joseph*

Cite This: *ACS Omega* 2024, 9, 41491−41503

Read Online

ACCESS | Metrics & More | Article Recommendations

ABSTRACT: Intraocular fungal infection poses a significant clinical challenge characterized by chronic inflammation along with vision impairment. Understanding the host defense pathways involved in fungal endophthalmitis will play a pivotal role in identifying adjuvant immunotherapy. Clinical isolates of *Candida albicans* (15,000 CFU/μL) were intravitreally injected in C57BL/6 mice followed by enucleation at 24 and 72 h postinfection. Histopathological analysis was performed to evaluate the retinal changes and the disease severity. RNA-seq analysis was conducted on homogenized eyeballs to assess the relevant gene profiles and their differentially expressed genes (DEGs). Pathway enrichment analysis was performed to further annotate the functions of the DEGs. Histopathological analysis demonstrated a higher disease severity with increased inflammatory cells at 72 hpi and transcriptome analysis revealed 27,717 DEGs, of which 1493 were significant (adj p value $\leq$0.05, FC $\geq$ 1.5). Among these, 924 were upregulated, and 569 were downregulated. Majority of the upregulated genes were associated with the inflammatory/host immune response and signal transduction and enriched in the T-cell signaling pathway, natural killer cell-mediated cytotoxicity, C-type receptor signaling pathway, and NOD-like receptor signaling pathway. Furthermore, inflammation-associated genes such as T-cell surface glycoprotein CD3, cathelicidin antimicrobial peptide, and lymphocyte cell-specific protein tyrosine kinase were enriched, while pathways such as MAPK, cAMP, and metabolic pathways were downregulated. Regulating the T-cell influx could be a potential strategy to modulate excessive inflammation in the retina and could potentially aid in better vision recovery in fungal endophthalmitis.

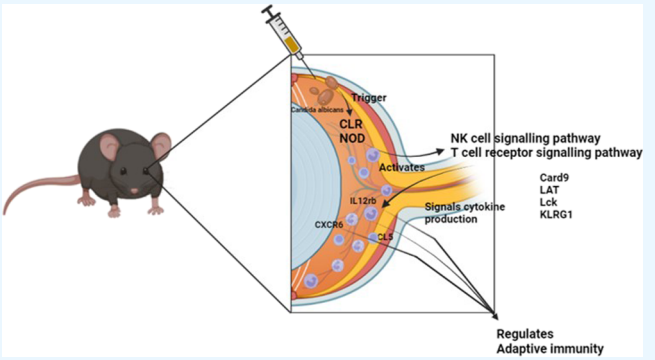

1. INTRODUCTION

Fungal endophthalmitis is a sight-threatening manifestation of intraocular infection characterized by chronic inflammation.[1,2] *Candida albicans* (C. albicans) is the predominant organism responsible for causing fungal endophthalmitis, especially in the West.[3] However, its dominance in India is not uncommon and is often associated with the higher rates of poor visual outcomes.[1] The infection presents a subacute onset as solitary, creamy chorioretinal infiltrates with symptoms worsening within days to weeks due to limited ocular space, delayed presentation of patients to the clinic, and misdiagnosis posing a considerable challenge for ophthalmologists.[4] With the progression of the condition, these lesions can extend into the vitreous chamber, resulting in symptoms such as blurred vision, floaters, vitreous opacities, and redness of the eye marked by the inflammatory clusters in the aqueous or vitreous chambers.[3−5] This leads to a heightened and uncontrolled inflammation outburst, where the specific toxic effects of the pathogen activate the inflammatory cascade causing an increased influx of inflammatory cells within the layers of the retina, leading to the disruption of its architecture paralleled with retinal function decline and vision loss.[6,7]

Although there are various classes of antifungals that are used in the treatment of fungal infections, only a few drugs are currently in use due to the limited availability of ophthalmic formulations.[6] Current therapeutic options employed for the treatment of fungal endophthalmitis typically include vitrectomy and intravitreal administration of antifungals such as amphotericin B, voriconazole, or fluconazole, depending on the susceptibility of the pathogen to the antifungals.[6,8]

Received: May 30, 2024
Revised: September 4, 2024
Accepted: September 17, 2024
Published: September 30, 2024

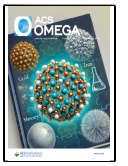

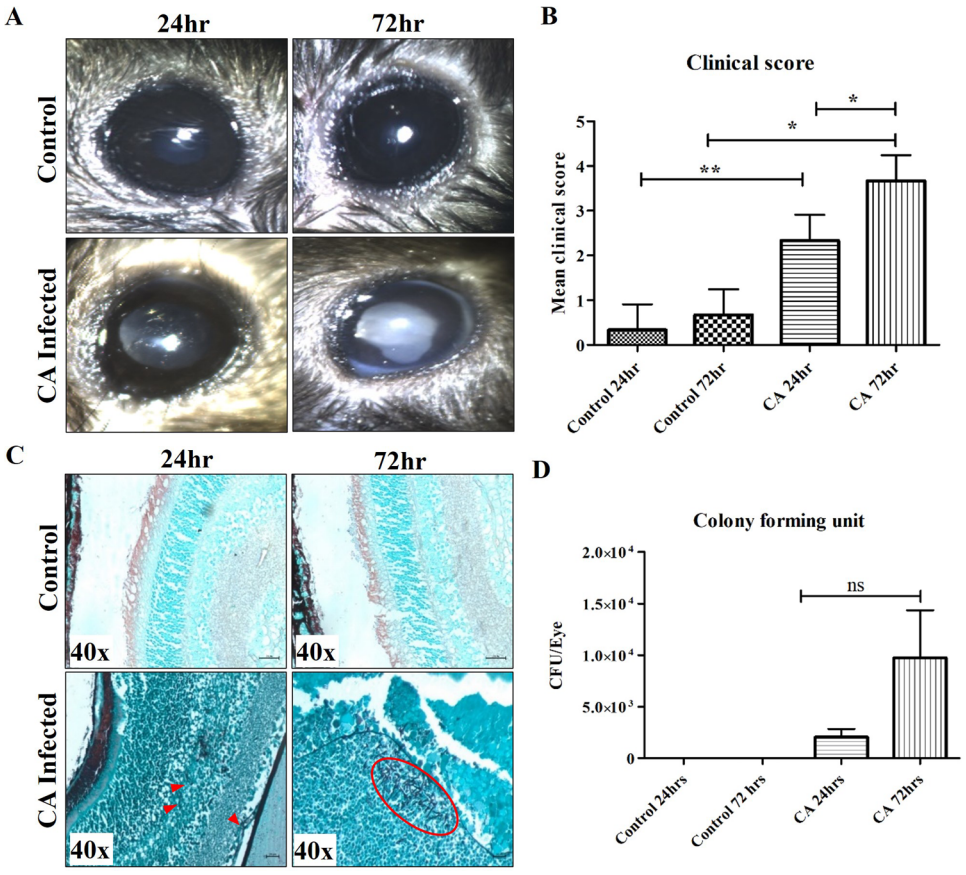

Figure 1. Phenotypic results (clinical, microbiological, and histopathological) following *C. albicans* infection in mice eye. (A) C57BL/6 mouse eyes were injected with 15,000 CFU/μL for 24 and 72 h. The ophthalmologist and pathologist, blinded to the infection type, scored the eyes and histopathological sections, respectively. (B) Clinical scores plotted as a bar graph. (C) GMS and (D) CFU was performed to check the purity and viability of the fungus. The graph represents the mean ± SEM. ns = not significant; *$p < 0.05$; and **$p < 0.01$. CA = *C. albicans*.

Moreover, in cases resistant to treatment, the repeated intravitreal administration of antifungals can escalate inflammation.[9] The utilization of intravitreal corticosteroids in fungal endophthalmitis is contentious due to concerns that they might compromise the effectiveness of antifungals, disrupt the immunogenic response, and potentially worsen the infection.[10] More research is clearly needed to explore the effects of corticosteroids in treating infectious endophthalmitis, as there is currently not enough evidence to determine their safety and effectiveness.[9,10] The management of endophthalmitis not only includes the clearance of infection but also emphasizes vision recovery. However, despite advancements in antifungal drugs and prompt treatment initiation, the progress in improving outcomes for fungal infections has been unsatisfactory.[1,11,12] This limitation can be attributed to the restricted efficacy of antifungal drugs in tackling infection without adequately addressing the heightened inflammation which is commonly seen in fungal infection.[11−13]

These findings highlight an urgent need to investigate targeted immunotherapeutic interventions as a safer approach to mitigate immunopathology during fungal endophthalmitis and improve vision recovery. Strategies focused on modulating the immune system or employing host-directed therapeutics to guide the host immune response and manage established infections offer promising avenues for exploration. Tramsen et al.[14] highlighted the potential use of antigen-stimulated T-cells in Aspergillus infection. Monoclonal antibodies such as Sulfasalazine, IgG, Mycograb, β-glucan-specific IgG2b, and various other antibodies have been evaluated against *Aspergillus* and *Candida* species, demonstrating immunomodulatory effects.[15−17] Additionally, Sionov and Segal (2003) described adjuvant therapy involving the enhancement of phagocytic function and bone marrow activity (myelopoiesis) using colony stimulating factors (CSFs) to treat invasive aspergillosis, leading to significantly improved treatment outcomes.[18,19] However, it is important to note that most of these therapies aim to boost the immune system for fungal infections throughout the body, whereas fungal endophthalmitis requires targeted and controlled immune suppression to preserve vision following fungal clearance.

In this study, transcriptomic and immunohistochemical profiling of *C. albicans* endophthalmitis in a C57BL/6 mouse model provided insights into the host immune response against fungal infection, and the pathways associated with inflammation were evaluated to comprehend disease pathobiology. These findings may serve as a basis for developing alternative or adjunctive treatment strategies for fungal endophthalmitis.

2. RESULTS

2.1. Clinical Assessment and Intraocular Fungal Burden Estimation of the Candida Endophthalmitis Mouse Model. A progressive increase in corneal opacity and the presence of hypopyon, angiogenesis, and intraocular inflammation were observed in the infected groups, while control eyes exhibited no visible signs of inflammation (Figure

https://doi.org/10.1021/acsomega.4c05081
ACS Omega 2024, 9, 41491−41503

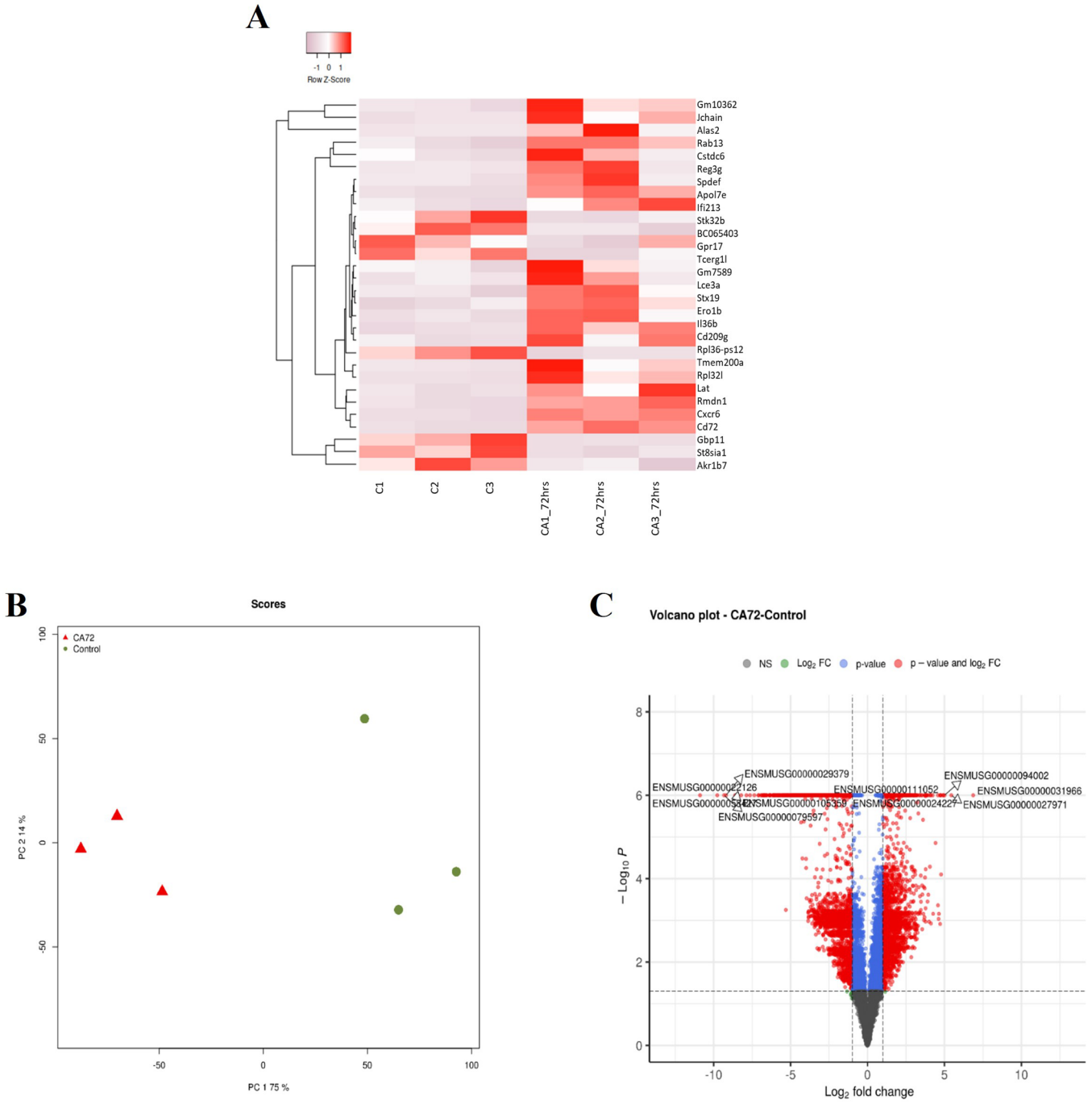

Figure 2. Results of the DEGs associated with fungal endophthalmitis. (A) Heatmap of the significant DEGs. Columns represent samples, and rows represent genes. Gene expression levels are shown on a scale with red signifying high expression levels and pink signifying low expression levels. (B) Principal component analysis (PCA) showing the biological replicates of the control (green) and CA-infected (red) mice eyes. (C) Volcano plot of significant DEGs between CA 72 h and the control. The *x*-axis denotes log2 fold change and the *y*-axis denotes $\log_{10}P$.

1A,B). After 48 h of inoculation, colonies of *C. albicans* appeared on the media, characterized by cream/white-colored smooth pasty colonies, confirming the presence and purity of *C. albicans* infection. The total number of *C. albicans* colonies per eye was higher at 72 h postinfection (9733 ± 4613) compared to 24 h (2033 ± 800) (Figure 1D), although this difference was not statistically significant (P = 0.17). This confirmed the establishment of a mouse model of *C. albicans* endophthalmitis. Additionally, the presence of intraocular fungal filaments within the vitreous cavity and along the margins of the retina was confirmed by Grocott's methenamine silver (GMS) stain (Figure 1C). Majority of the 24 h *C. albicans*-infected eyes presented with the clinical scoring of 2−3, which attributed to an obvious flare with 10−50 cells/field, mild to moderately diminished red reflex, and mild to moderate vitreous and retinal clarity; the clinical presentation also matched with that of the patients presented at our institute. However, at 72 h postinfection, the clinical signs were relatively more prominent with an intense flare above 50 cells/field, moderate to no red reflex, and details of retina completely obscured.

https://doi.org/10.1021/acsomega.4c05081
ACS Omega 2024, 9, 41491−41503

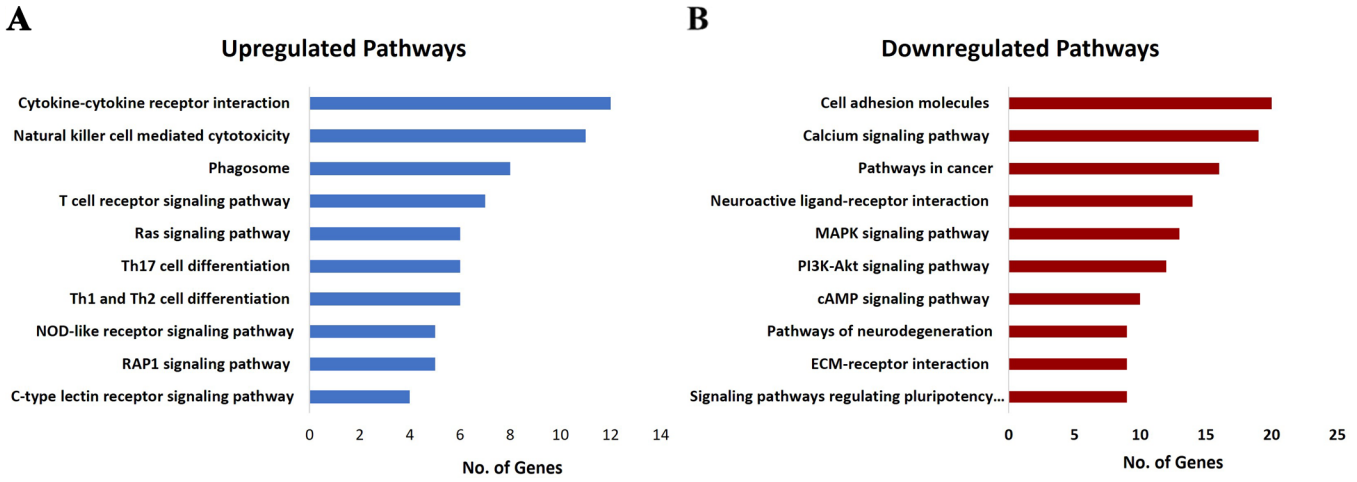

Figure 3. KEGG pathway analysis of the (A) upregulated and (B) downregulated genes. The bars indicate the number of genes enriched in each pathway. The *x*-axis represents the number of genes, and the *y*-axis represents the KEGG pathway terms.

2.2. DEGs Distinctively Classified the Transcriptome Profiles of *C. albicans* Infected from the Control. We identified a total of 27,179 gene transcripts. Subsequently, by comparing the patterns of gene expression between the CA-infected and control groups and applying the criteria of FDR < 0.1%, a $\log_2$ fold change $\geq$1.5, and a significance level of $p \leq 0.05$, we identified 1493 differentially expressed genes. Among these, 924 genes were upregulated, while 569 genes were downregulated. The gene expression levels are represented on a heatmap scale, where red and pink indicate high and low expression levels, respectively. PCA revealed a strong correlation between biological replicates, which highlights the distinct expression signatures between the infected and control groups (Figure 2B). A volcano plot was constructed to visualize changes in gene expression between the control and infected groups (CA 72 h), highlighting genes with statistically significant differences $p \leq 0.05$, as shown in Figure 2C.

The top KEGG pathway enrichments among the upregulated DEGs included cell adhesion molecules, cytokine-cytokine receptor interaction, natural killer cell-mediated cytotoxicity, phagosomes, T-cell receptor signaling pathways, oxidative phosphorylation, Th17 cell differentiation, Th1 and Th2 cell differentiation, and Ras signaling pathways. And the downregulated DEGs were associated with metabolic pathways, cell adhesion molecules, calcium signaling pathways, PI3K-Akt signaling pathways, MAPK signaling pathways, and cAMP signaling pathways (Figure 3A,B).

2.3. Transcriptomic Profiling Shows a Delicate Interplay between Innate and Adaptive Immunity in Candida Endophthalmitis. We further explored the function of the significant DEGs, which could potentially play a crucial role in the pathogenesis of *C. albicans* endophthalmitis by regulating specific signature pathways. The C-type lectin receptor signaling pathway was observed to be modulated by several genes: C-type lectin domain family 4 member b1, C-type lectin domain family 1 member b, PYD and CARD domain, killer cell lectin-like receptor family I, killer cell lectin-like receptor subfamily C, and member 1 and calmodulin 4. C-type lectin receptors (CLRs) belong to a group of pattern recognition receptors (PRRs) crucial for defending against invasive fungal infections. Other PRRs such as the NOD-like receptor were also elevated with genes such as the apoptosis-associated speck-like protein containing a CARD, baculoviral IAP repeat-containing protein 1, and cathelicidin antimicrobial peptide, which were also associated with the toll-like receptor signaling pathway. Numerous cell surface molecules exhibited significant upregulation, including CD22 antigen, CD72 antigen, CD79A antigen (immunoglobulin-associated α), and CD79B antigen. These molecules are pivotal in activating antigen-presenting cells such as natural killer cells and B-cells. Additional genes associated with natural killer cell-mediated cytotoxicity were lymphocyte cell-specific protein tyrosine kinase, ribosomal protein S17 pseudogene, killer cell lectin-like receptor subfamily C1, and killer cell lectin-like receptor subfamily K member 1. Furthermore, the upregulation of genes such as CD3 antigen delta polypeptide, CD3 antigen γ polypeptide, lymphocyte protein tyrosine kinase, and interleukin 12 receptor β 1 likely contributed to the activation of adaptive immunity by initiating T-cell receptor signaling, Th1 and Th2 cell differentiation, and Th17 cell differentiation. Additionally, other genes such as T-cell surface glycoprotein CD3 delta chain, T-cell surface glycoprotein CD3 γ chain, T-cell surface glycoprotein CD8 α chain, T-cell surface glycoprotein CD8 β chain, lymphocyte cell-specific protein tyrosine kinase, T-cell receptor β variable 3 T-cell receptor-associated transmembrane adapter 1, T-cell receptor β variable 10, T-cell receptor β variable 12−2, T-cell receptor β variable 13−1, selection and upkeep of intraepithelial T-cells 3, T-cell receptor β constant region 1, T-cell receptor γ variable 6, T-cell receptor β variable 1, and T-cell receptor β variable 2 observed in our study were also reported to regulate the T-cell activation. We also observed the upregulation of genes such as Linker for activation of T-cells, lymphocyte antigen 6 complex locus M, lymphocyte antigen 6 complex locus D,[20,21] lymphocyte protein tyrosine kinase, lymphocyte antigen 9, and lymphocyte antigen 86, which are associated with the Rap1 signaling pathway.

Furthermore, transcriptomic profiling also identified crucial genes such as tumor necrosis factor (ligand) superfamily member 13, tumor necrosis factor receptor superfamily member 25, tumor necrosis factor α-induced protein 8-like 2, phospholipase A2 group IID, calcium/calmodulin-dependent protein kinase I γ, phospholipase A2 group IVF, immunoglobulin kappa variable 1−110, immunoglobulin kappa variable 3−12, small proline-rich protein 2H, CD160 antigen, apolipoprotein L 7e, regenerating islet-derived 3 γ,

https://doi.org/10.1021/acsomega.4c05081
ACS Omega 2024, 9, 41491−41503

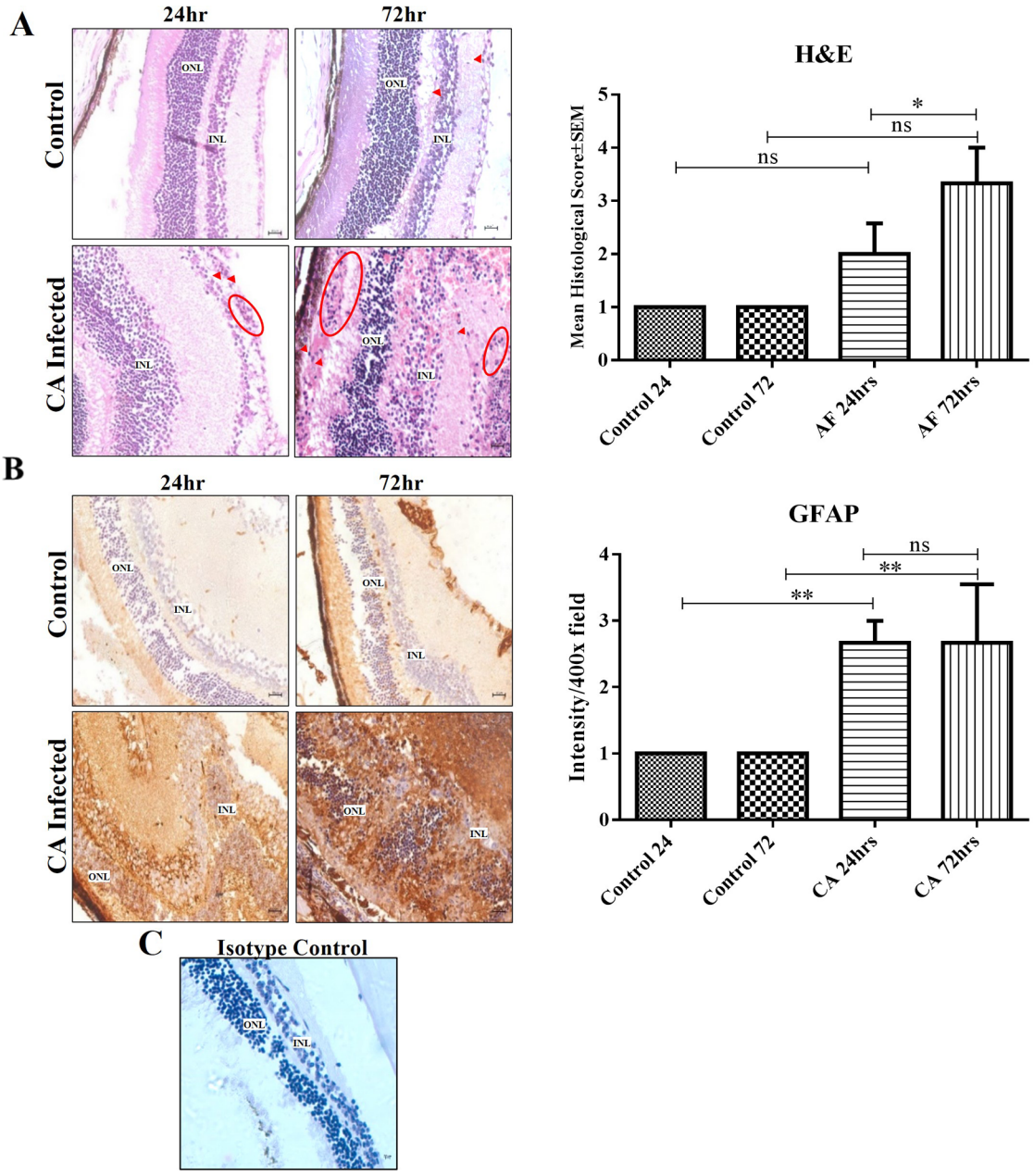

Figure 4. Representative H&E- and GFAP-stained sections. C57BL/6 mouse eyes were injected with 15,000 CFU/μL for 24 and 72 h. A pathologist, blinded to the study, analyzed three randomly picked fields within a tissue section. (A) H&E staining was performed and the disease severity was assessed. Red circles and arrowheads indicate the influx of inflammatory cells. ONL, outer nuclear layer; INL, inner nuclear layer. (B) Quantification of the GFAP intensity under a high-power field. (C) Isotype control (IgG). The graph represents mean ± SEM. The unpaired *t* test was used to calculate the significance. Original magnification, ×400. ns = not significant; *$p \leq 0.05$; and **$p \leq 0.01$. CA = *C. albicans*.

chemokine (C−C motif) ligand 21A (serine), chemokine (C-X-C motif) receptor 6, guanine nucleotide binding protein (G protein), γ 11, platelet factor 4, and chemokine (C−C motif) ligand 5, which could possibly play a significant role in directing the host immune response or pathogen elimination.

Genes like aldo-keto reductase family 1 member B7, aldehyde oxidase 2, D-amino acid oxidase, amine oxidase copper-containing 2 (retina-specific), tyrosine hydroxylase, polypeptide *N*-acetylgalactosaminyltransferase 17, β-1,3-glucuronyltransferase 1 (glucuronosyltransferase P), phosphodiesterase 4C cAMP specific, transmembrane protein 86B, and dual specificity phosphatase 9 were downregulated, which are associated with metabolic pathways, along with Fibroblast growth factor 14, fibroblast growth factor receptor 4, FBJ osteosarcoma oncogene, glial cell line-derived neurotrophic factor, glial cell line-derived neurotrophic factor associated with the MAPK signaling pathway and the Pi3K/Akt pathway. Additionally, one of the prominent gene mitogen-activated protein kinase 21, associated with the MAPK pathway, was also found to be downregulated. Other genes like Serine/threonine kinase 32B, G protein-coupled receptor 17, transcription elongation regulator 1-like, transmembrane protein 200A, matrix metallopeptidase 24, insulin receptor-related receptor, cannabinoid receptor 1 (brain) (−1.7), kinase suppressor of ras 2, glutamate receptor, ionotropic, NMDA2B (epsilon 2), solute carrier family 25 (mitochondrial oxodicarboxylate

https://doi.org/10.1021/acsomega.4c05081
ACS Omega 2024, 9, 41491−41503

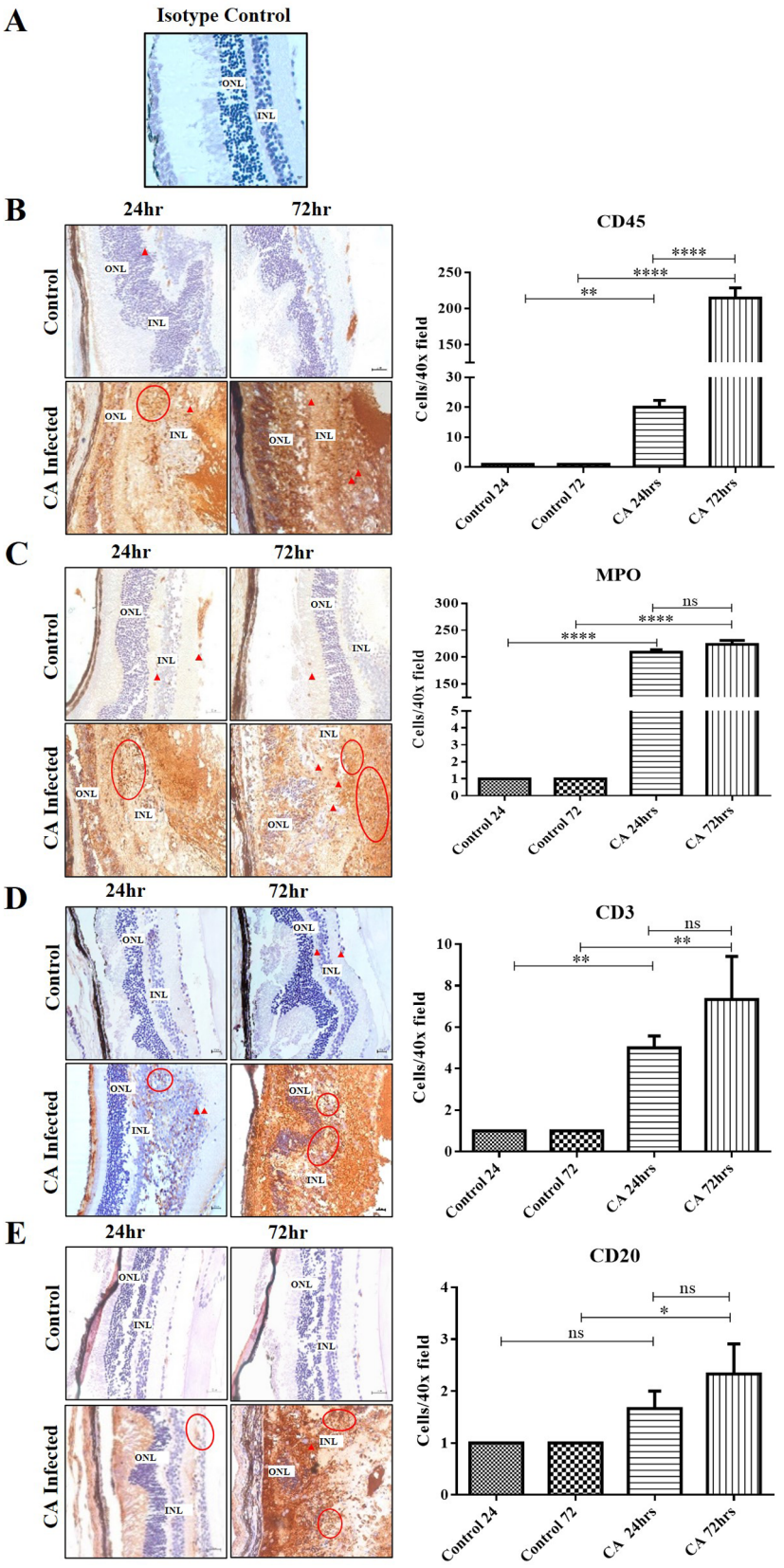

Figure 5. Immunohistochemical examination of the mice eyeballs. C57BL/6 mice eyes were injected with 15,000 cells of *C. albicans*. For histological assessment, infected eyes together with the vehicle control were harvested. The tissue sections were stained with (A) the isotype control (IgG), (B) CD45, (C) MPO, and (D) CD3 and (E) CD20. Red circles and arrowheads indicate the positive cells. The positive cells were counted, and the mean ± SEM values were represented as bar graphs. Pictures are the representation of one of the biological replicates, and graphs represent the collective data of 3 independent experiments where $n = 3$ in each group. Original magnification, ×400; ns = not significant; *$p \leq 0.05$; **$p \leq 0.01$; and ***$p \leq 0.001$. CA = *C. albicans*.

https://doi.org/10.1021/acsomega.4c05081
ACS Omega 2024, 9, 41491−41503

carrier), and member 21 were found to be significantly downregulated.

2.4. Histopathological Evaluation Confirms the Increased Influx of Inflammatory Cells and Retinal Stress (GFAP). Histological examination was performed to further assess the disease progression; this revealed a time-dependent increase in inflammatory cells, retinal folding, and disruption of the retinal structure. The disease severity and notable inflammation increased at 24 h, though not significant ($p = 0.2879$), but we observed a significant increase at 72 h ($p = 0.0257$) (Figure 4A). Subsequently, we assessed the intensity of glial fibrillary acidic protein (GFAP) at both time points to potentially correlate the disease severity with the retinal stress (Figure 4B). We observed a significant increase in the retinal stress in the Candida-infected eye when compared to the control at both 24 h ($p = 0.0075$) and 72 h ($p = 0.0075$).

2.5. Excessive Host Immune Response in *C. albicans*-Induced Endophthalmitis. To assess the infiltration of inflammatory cells at 24 and 72 hpi, we counted the number of CD45, MPO, CD3, and CD20 cells in the posterior segment of the eye. The number of CD45+ ($p = 0.0001$), a leukocyte marker, and MPO ($p = 0.08$), a neutrophil marker, displayed progressive increase over time from 24 to 72 hpi. While CD3, a T-cell marker, showed a time-dependent elevation, ($p = 0.0474$) CD20 ($p = 0.2302$), a B-cell marker, did not exhibit a statistically significant increase, suggesting that T-cells are primarily involved in the adaptive immune response during *C. albicans* endophthalmitis (Figure 5). Table 1 elucidates the histopathological grading ranging from 0 to 4+ based on the severity of inflammation observed in the posterior and retinal chambers.[22]

2.6. *C. albicans* Endophthalmitis Induces Pronounced Cell Death in C57BL/6 Mice. To correlate the clinical and immunohistochemistry findings, a TUNEL assay was performed. We observed the significant increase ($p < 0.0001$) in the retinal cell death at 72 hpi (82.3 ± 43.7 apoptotic cells) when compared to 24 hpi (27.6 ± 14.6 apoptotic cells), which in turn is comparable with the increased disease severity and fungal burden seen in the clinical and histopathological examination. Majority of the cell death was observed in the inner and the outer nuclear layer of the retina. Retinal cell death accompanied by a robust inflammatory cell influx could potentially contribute to a larger extent of vision loss (Figure 6).

2.7. Quantification of the T-Cell Subset. In order to confirm the infiltration of T-cells at 24 and 72 hpi, we quantified the presence of CD4- and CD8-positive cells. The number of CD4-positive cells a helper T-cell marker showed a significant increase at 24 h when compared to the control ($p = 0.0001$) and 72 hpi ($p = 0.0213$). Conversely, CD8, a marker for cytotoxic T-cells, demonstrated a gradual increase over time compared with the control ($p = 0.0005$) and between 24 and 72 hpi ($p = 0.0001$) (Figure 7).

3. DISCUSSION

Intraocular fungal infection is a vision-threatening complication characterized by chronic inflammation due to an uncontrolled immune response from the host.[4,9,23] While inflammation is essential for controlling the infection, it can also harm the eye by the excessive influx of inflammatory cells and molecules, potentially leading to irreversible vision damage by disrupting the retinal structure.[13] Understanding the host-mediated immune response to fungal endophthalmitis is

Table 1. Histopathological Evaluation of the Murine Model of Endophthalmitis (Adapted from Ramadan et al., 2006)

score	0	1+	2+	3+	4+
inflammation (posterior chamber)	no presence of infiltrating inflammatory cells	no fibrin was observed, 1−10 infiltrating cells per field	presence of 10−50 infiltrating cells per field, mild fibrin reaction observed	significant fibrin reaction was observed with 50−100 infiltrating cells per field	both regions exhibit fibrinous and cellular infiltration
retinal architecture	completely intact retina	<25% retinal folds of the retina	retinal folds and detachment in 25−50% of the retina	retinal folds and detachment in 50−75% of the retina	complete detachment, retinal layers indistinguishable

https://doi.org/10.1021/acsomega.4c05081
ACS Omega 2024, 9, 41491−41503

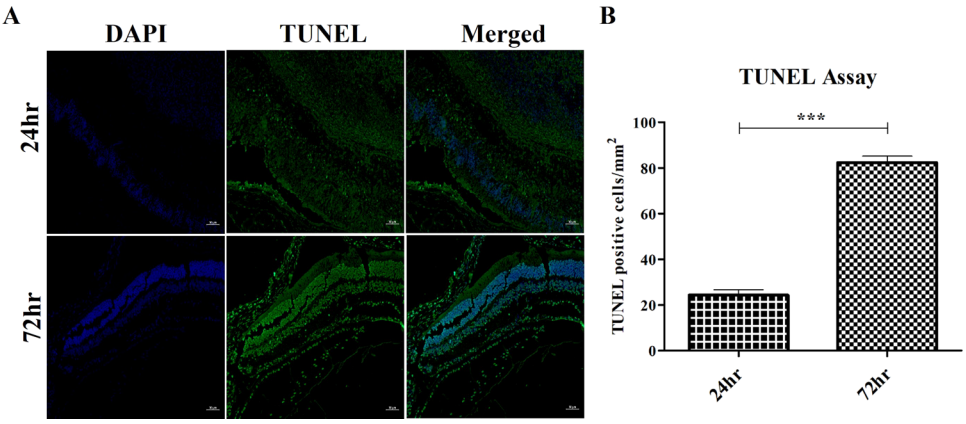

Figure 6. Retinal cell death observed in C57BL/6 mice eyes infected with *C. albicans*. Infected eyes were enucleated at 24 and 72 hpi for histological examination. (A) Apoptosis in the retina was assessed using a TUNEL-based assay, followed by counterstaining with 4′-6-diamino-2-phenylindole (DAPI). (B) Graph representing the number of TUNEL-positive cells. ****$p \leq 0.0001$.

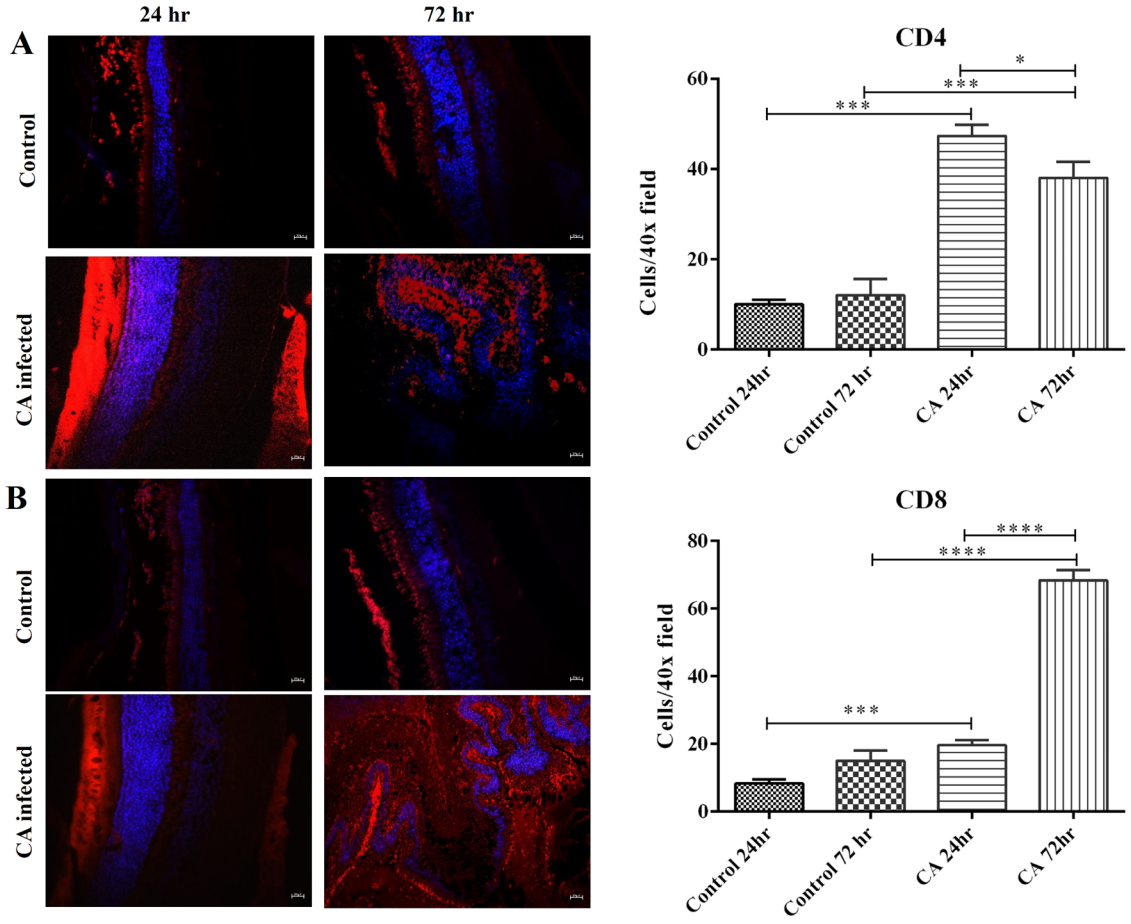

Figure 7. Validation of association of T-cells in fungal endophthalmitis. The tissue sections were stained with (A) CD4 and (B) CD8 in red and the nucleus was stained with DAPI blue. The positive cells were counted and the mean ± SEM values were represented as bar graphs. Original magnification, ×400. ns = not significant; *$p \leq 0.05$; ***$p \leq 0.001$; and ****$p \leq 0.0001$.

essential for refining treatment strategies and facilitating visual recovery. This study delves into the intricate transcriptional patterns to uncover fungal pathogenesis and identify gene expression alterations, particularly in a mouse model infected with *C. albicans* endophthalmitis.[9,24] While previous research on fungal infections, especially in ocular contexts, typically emphasizes the role of the innate immune system and overall inflammation, our investigation offers a thorough examination of transcriptional profiles.[25] Importantly, we examined not only the initial response but also the involvement of the adaptive immune system (specifically T-cells) and its associated gene signatures. Additionally, we elucidate the underlying mechanisms of these interactions and their repercussions on the mouse retina.

Comparative transcriptional profiling reveals the striking elevation in the transcriptomic magnitude exclusively of

https://doi.org/10.1021/acsomega.4c05081
ACS Omega 2024, 9, 41491−41503

inflammatory mediators and inflammation-associated pathways such as natural killer cell-mediated cytotoxicity, cytokine−cytokine receptor interaction, metabolic pathways, C-type lectin receptor signaling pathway, T-cell signaling pathway, phagosome, NOD-like receptor signaling pathway, Th1 and Th2 cell differentiation, and Th17 cell differentiation. Several genes associated with these pathways interact, initiating the activation of the whole cascade of inflammatory responses, and the genes showing the biggest differences in expression levels were those most critical for the T-cell immune response against *C. albicans*. C-type lectin receptors play a major role in regulating antifungal immunity signaling cascades and induce an adaptive immunity response to pathogens, and C-type lectin receptor signaling pathway-associated genes such as C-type lectin domain family 4 member b1, C-type lectin domain family 1 member b, and the PYD and CARD domains identified in our study are known to participate in antigen uptake at the infection site, either for eliminating the antigen or for its processing and subsequent presentation to T-cells.[26−28] NOD-like receptor activation can provide costimulatory signals alongside antigen presentation by antigen-presenting cells (APCs) to T-cells. This costimulation can enhance T-cell activation and proliferation.[29] Additionally, we also observed the elevation of the RAP1 signaling pathway, which is a key regulator of T-cell and antigen-presenting cell interactions further modulating T-cell responses.[30]

Majority of the pathways identified in our study directly or indirectly contribute to activation of cell-mediated immunity, especially CD8+ T-cell activation during fungal endophthalmitis. We also observed several T-cell pathway-mediated genes such as the T-cell surface glycoprotein CD3 delta chain and γ chain, lymphocyte cell-specific protein tyrosine kinase, T-cell receptor β variable 3, and T-cell receptor-associated transmembrane adapter 1. The increased levels of the T-cell surface glycoprotein CD8 α chain and T-cell surface glycoprotein CD8 β chain are indicative of the involvement of cytotoxic T-cells in fungal endophthalmitis. Additionally, genes such as neutrophil cytosolic factor 1 is reported to promote autoreactive CD8+ T-cell activation, and tyrosine-protein kinases, which are involved in signals mediated by various cytokines or antigen receptors, also play a prominent role in T-lymphocyte activation and differentiation.[31−33] Furthermore, the elevation of genes such as granzymes (A, E, K) and natural killer cell group 7 suggests that the cytotoxic cells such as CD+ T-cells and NK cells could possibly employ a granzyme-dependent pathway to eliminate infected cells.[34] We also observed the increased levels of signaling lymphocytic activation molecule Family 7 (SLAMF7), which plays a key role in reprogramming the Treg cells.[35] Although B-cell-associated CD antigens such as CD22, CD72, CD79A, and CD79B were identified in the transcriptomic studies, our study did not find strong evidence of genes directly involved in B-cell activation. This suggests that B-cells might either be involved at a different stage of the infection or play a less important role in *C. albicans* endophthalmitis. Our findings are consistent with the histopathological observations, which showed a small but significant increase in B-cells only at 72 h, while T-cells showed a significant rise at both 24 and 72 h postinfection.

The genes plotted in the heatmap like Linker for activation of T-cells (LAT) play a critical role in adaptive immunity in T-cell activation and differentiation.[36,37] IL-36 acts as a key regulator in the early phases of the immune response by triggering the production of IFNs and promoting the recruitment of immune cells.[38] CXCR6 helps identify resident memory T-cells (TRM cells). TRM cells play a vital role in immunosurveillance by interacting with epithelial cells, the frontline defense of our tissues.[39] Other genes related to the host immune response includes β-defensins, which are antimicrobial peptides active against various fungal infections, especially Candida species.[40] Interestingly, however, we observed the downregulation of PI3K-Akt and MAPK pathways known to regulate T-cell differentiation and activation. Although we did not find genes that are directly implicated in the regulation of these pathways, we identified genes such as tenascin, fibroblast growth factor, and integrins that are known to be associated with these pathways according to the KEGG pathway analysis. Src kinase-associated phosphoprotein 1, a negative regulator of T-cell activation, was upregulated.

While fungal endophthalmitis triggers a strong inflammatory response with T-cell activation, influx of immune cells into the immune-privileged environment of the eye can unfortunately lead to retinal damage and vision loss.[41,42] Finding ways to improve vision recovery is crucial for managing endophthalmitis. Our comprehensive transcriptomic analysis suggests that diacylglycerol kinase might be a target for immunotherapy, potentially mitigating the immunogenic response.[43] Additionally, the drug cyclosporine A, which suppresses the immune system, has been shown to selectively target T-cell activation with minimal impact on other immune cells and phagocytic cells, which could help regulate excessive inflammation. Interestingly, it is also reported to have antifungal activity especially on Candida *spp.*, rendering it as a favorable therapeutic option.[44] A schematic diagram, as depicted in Figure 8, summarizes the key findings of this study.

4. CONCLUSIONS

Overall, the transcriptional profiling of Candida endophthalmitis demonstrated significant temporal changes in gene expression between the control, 24 h postinfection samples, and 72 h postinfection samples. While there was predominant

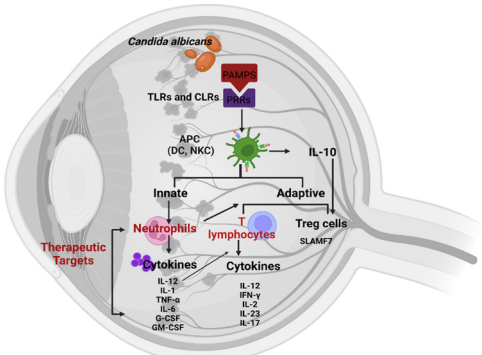

Figure 8. Schematic representation of pathologic insights into Candida endophthalmitis. The pathogen-associated molecular patterns (PAMPs) are recognized by host pathogen recognition receptors (PRRs) which further activate antigen-presenting cells (APCs) like dendritic cells (DCs) and natural killer cells (NKCs). This will lead to a series of cascadic events in turn activating innate and adaptive immune responses, and an exacerbated inflammation with inflammatory mediators such as cytokines and chemokines is observed in the posterior part of the eye. Neutrophils and T-lymphocytes could be potential therapeutic targets to regulate inflammation and salvage the vision.

https://doi.org/10.1021/acsomega.4c05081
ACS Omega 2024, 9, 41491−41503

activation of innate immune responses at 24 h postinfection, by 72 h postinfection, there was not only a sustained innate immune response, notably involving neutrophils, but also a marked increase in the adaptive immune activity involving predominantly cytotoxic T-cells. This dynamic interplay between innate and adaptive immunity highlights the evolving nature of the host defense mechanisms against Candida endophthalmitis over time. Additionally, targeting neutrophils and T-cells with immunomodulators as therapeutic strategies to control inflammation and prevent collateral damage presents a promising approach to manage fungal endophthalmitis.

5. MATERIALS AND METHODS

5.1. Ethics Statement. C57BL/6 mice (mixed gender, 6−8 weeks old) were used for the study. The mice were treated in accordance to the guidelines outlined by the Association for Research in Vision and Ophthalmology (ARVO) statement for the ethical use of animals in ophthalmic and vision research. The study was approved by the Institutional Animal Ethics Committee (IAEC), Vyas Laboratories, Hyderabad, India (protocol approval number IAEC/VL/08/2022−23).

5.2. Fungal Culture Preparation. For this study, the *C. albicans* (L-614/2017) strain was isolated from the vitreous chamber of patients diagnosed with *C. albicans* endophthalmitis. The strain was cultured in potato dextrose agar and maintained for 24−48 h at 37 °C. The yeast cells were suspended in sterile phosphate-buffered saline (pH = 7.2) and quantified using a hemocytometer to obtain the final concentration of 15,000 cells/μL.

5.3. Establishment of the Mouse Model. As detailed in the prior study, mice (C57BL/6) were anesthetized using a combination of ketamine and xylazine along with the topical anesthetic proparacaine (0.5%). Eyes were disinfected with 10% betadine and dilated with 1% tropicamide for better visualization during intraocular injections.[45] Mice were intravitreally injected with 15,000 CFU/eye of *C. albicans* (CA) into the mid-vitreous through the posterior limbus, and the contralateral eye was injected with sterile phosphate-buffered saline (PBS), which served as the control, and monitoring was done daily for up to 72 h using a hand-held slit-lamp to track the development of infection. Throughout the course of infection establishment and progression, eyes were clinically examined by an ophthalmologist blinded to the type of infection. Following 24 and 72 h postinfection, mice were euthanized and eyeballs were carefully plucked out from the eye socket with a pair of forceps and were immediately washed with sterile 1× PBS and stored in appropriate different storage solutions according to the downstream processes. For the whole transcriptome analysis, the enucleated eyes were collected in RNA later and stored at −80 °C and for histopathological analysis, they were fixed in 10% formalin. Similarly, for the CFU, the eyeballs were stored in 1× sterile PBS (pH = 7.2).

5.4. RNA Sample Preparation and Sequencing. Total RNA was extracted from the mice eyeballs (n = 3) using RNeasy mini kits (Qiagen) following the manufacturer's instruction, followed by DNase treatment (Thermo Scientific). The concentration of RNA was assessed by NanoDrop (Biorad) and the quality was estimated by Tapestation 4200 (Agilent Technologies, Santa Clara). The samples with a RIN of ≥7 were selected for transcriptomics.

Following the cDNA synthesis, libraries were prepared (KAPA mRNA capture kit) and sequenced on Illumina Nextseq 2K, which generated 40M, 2 × 150 bp reads/sample. FASTQ files were generated from the sequenced data, which were then considered for further processing.

5.5. RNA-seq Alignment and Analysis Pipeline. Global transcriptome analysis was performed using RNA-seq to elucidate the host immune response of *C. albicans* infection at the molecular level. We selected a time point (72 h postinfection) where there was an active infection induced by *C. albicans* through alignment with the *Mus musculus* reference genome (mm8 https://genome.ucsc.edu/cgi-bin/hgTracks?db=mm10&chromInfoPage=). Prior to analysis, the quality of the paired-end raw sequencing reads was evaluated. Subsequently, Trimmomatic was employed to trim low-quality sequences (phred score $Q < 33$) and remove adapter contamination. Trimmed sequence reads are mapped to the reference transcriptome with HISAT2. FeatureCounts was used to obtain feature-specific expression counts, and low count features across samples were detected and removed using the Limma-Voom package. Expression count normalization was performed with the TMM method from Limma-Voom. Estimation of significant differential features was performed with Limma-Voom, which simulates technical replicates for data. We performed heatmap analysis to illustrate the expression patterns of these sets of differentially expressed genes. Following the stringent filtering of the data, top 20 significant DEGs presumed to play a crucial role in the host immune response in Candida endophthalmitis were represented in the heatmap along with their expression trends. The heatmap was generated using the heatplot function from the made4 R package for top upregulated and downregulated features based on $\log_2$FC. In order to understand the different characteristics between the healthy control and the *C. albicans*-infected group, we constructed principal component analysis (PCA) of the differentially expressed genes. A volcano plot was generated with the EnhancedVolcano R package. The criteria for screening DEGs were selected as $\log_2$ fold change ≥1.5 and adj $p \leq 0.05$. The R package was used using R studio software (version 4.3.1).

5.6. Pathway Enrichment Analysis. In order to analyze the molecular functions of the DEGs, pathway enrichment was performed using the KEGG database. KEGG pathway enrichment analysis determined the metabolic and signaling pathways, where the differentially expressed genes were primarily involved. To identify the DEGs, we applied strict selection criteria. Genes were considered significant DEGs if their threshold values were FDR < 0.1, fold change as $\log_2$ fold change ≥1.5, and $p < 0.05$. Following the stringent selection of DEGs, the genes were analyzed for enriched pathways through the Kyoto Encyclopedia of Genes and Genomes and the top 20 enriched pathways were selected based on the number of genes associated with the pathways. Among these, top host−pathogen interaction- and inflammation-associated pathways were plotted on the graph. These selection criteria highlight the critical involvement of pathways such as the cytokine−cytokine receptor interaction, natural killer cell-mediated cytotoxicity, T-cell receptor signaling pathway, cell adhesion molecules, calcium signaling pathway, and neuroactive ligand−receptor interaction in the pathobiology of *C. albicans* endophthalmitis. To ensure the accurate mapping of DEGs to the KEGG database for *M. musculus*, official gene symbols were used as unique identifiers. This mapping process allowed us to generate a functional annotation chart highlighting the significantly enriched pathways within the KEGG database.

https://doi.org/10.1021/acsomega.4c05081
ACS Omega 2024, 9, 41491−41503

5.7. Histopathology and Immunohistochemistry Analysis. Enucleated mice eyeballs at desired time points were fixed in 10% neutral buffered formalin and embedded on paraffin blocks, and 4 μm sections were taken and stained with the haematoxylin and eosin (H&E) stain to check the disease severity. Further sections were stained with Grocott's methenamine silver (GMS) stain to check the fungal burden and for other inflammatory markers like the T-cell marker (CD3), B-cell marker (CD20), leukocyte marker (CD45), neutrophil marker (MPO), and astrocyte and Muller glia marker (GFAP), and they were examined under an Olympus light microscope (BX51). In brief, the procedure included deparaffinization of all 4 μm thick paraffin sections of mice eyeballs with xylene, and graded alcohol of 100, 90, and 80% dilutions was used to rehydrate the sections. Following incubation with primary antibodies and further incubation with 2° antibodies (Dako, Agilent, Santa Clara, CA), the sections were washed with PBS three times, following incubation for 5 min with the DAB substrate (catalog no. HK124-9K, BioGenex, CA), washing with distilled water, and counterstaining with Harris's hematoxylin. Lastly, the slides were mounted and assessed for the number of positive cells in the posterior chamber by taking the average of 5 random microscope fields per case at ×400 magnification. Histopathological evaluation was performed by a pathologist who was blinded to the study type and the nature of the infection. The severity of the infection was assessed by different parameters such as inflammation in the posterior segment and integrity of the retinal architecture and score 0 was attributed to no infiltrating inflammatory cells and intact retinal architecture, while score 4 was attributed to 100+ inflammatory cells and indistinguishable retinal layers. The histopathological scoring was done as described previously by Rudraprasad et al.[45] Table 2 describes the details of the antibodies used in this study.

Table 2. List of antibodies

antibodies	catalog number	supplier
CD45	M0701	Dako
MPO	A0398	Dako
CD3	M7254	Dako
CD20	M0755	Dako
GFAP	Z0334	Dako
IgG	E20-V	Vitro Master
CD4	MT310	Santacruz
CD8	32-M4	Santacruz

5.8. Tunnel Assay. Apoptosis was determined using a TUNEL assay-based procedure (Click-iT TUNEL Alexa Fluor 488, Thermo Fisher Scientific, Waltham, MA) within the retinal tissue, and the nuclei were stained with DAPI. DNase I enzyme served to induce DNA strand breaks, resulting in a TUNEL-positive reaction. Subsequently, coverslips were rinsed using molecular biology-grade water. Following this step, a reaction blend was created utilizing deionized water, DNase I buffer, and DNase I. Altogether, 100 μL of the reaction mixture was applied to the coverslip and allowed to incubate at room temperature for 30 min. After incubation, the coverslips were again washed using deionized water and subjected to the TdT reaction.[46] The proportion of TUNEL-positive cells was analyzed by ImageJ after taking photos with a microscope. Images were obtained under an ×20/0.8 lens with the help of an AXIO Imager.M2 Zeiss fluorescence microscope.

5.9. Immunofluorescence Assay. Immunofluorescence assays were conducted to confirm the involvement of T-cells in Candida endophthalmitis. Slides were prepared and deparaffinized using the same procedure as that for immunohistochemistry. Antigen retrieval was performed using citrate buffer (pH 6.0) with multiple cycles of heating (420 W for 5 min per cycle). Phosphate-buffered saline (PBS, pH 7.2) was utilized for washing the sections three times for 5 min each, followed by permeabilization with Triton-X (0.3%) at room temperature. Blocking was carried out using 2.5% bovine serum albumin (BSA) prepared in PBS (pH 7.4; filtered with a PES 0.22 sterile filter [GVS Filtrations]) for 45 min. Subsequently, the tissue sections were incubated with CD4 and CD8 antibodies (Dako GA511) prepared in 1% BSA. A secondary antibody (1:500; A11012, Invitrogen) was applied and incubated for 45 min. The slides were then mounted with DAPI (4, 6-diamidino-2-phenylindole; ab104139, Abcam) for nuclear staining. Slide examination was conducted by using a fluorescent microscope (Carl Zeiss, Axio Scope A1).

5.10. Statistical Analysis. Prism 6 (GraphPad Software Inc., San Diego, CA) was used for the statistical analyses and graphical representations. R scripts were used to construct volcano plots, and the online tool Heatmapper was used to obtain the heatmap. All of the experiments were performed with at least 3 biological and 3 technical replicates. Differences in the means were calculated using the two-tailed unpaired t test considering $p > 0.05$, ns (nonsignificant); *$p \leq 0.05$; **$p \leq 0.01$; ***$p \leq 0.001$; and ****$p \leq 0.0001$.

AUTHOR INFORMATION

Corresponding Author

Joveeta Joseph − *Jhaveri Microbiology Centre, Brien Holden Eye Research Centre, LV Prasad Eye Institute, Hyderabad 500034 Telangana, India;* orcid.org/0000-0002-8421-1977; Phone: 91-40-68102517; Email: joveeta@lvpei.org

Authors

Agimanailiu Khapuinamai − *Jhaveri Microbiology Centre, Brien Holden Eye Research Centre, LV Prasad Eye Institute, Hyderabad 500034 Telangana, India; Center for Doctoral Studies, Manipal Academy of Higher Education, Karnataka 576104, India*

Dhanwini Rudraprasad − *Jhaveri Microbiology Centre, Brien Holden Eye Research Centre, LV Prasad Eye Institute, Hyderabad 500034 Telangana, India; Center for Doctoral Studies, Manipal Academy of Higher Education, Karnataka 576104, India*

Suchita Pandey − *Jhaveri Microbiology Centre, Brien Holden Eye Research Centre, LV Prasad Eye Institute, Hyderabad 500034 Telangana, India*

Dilip Kumar Mishra − *Ocular Pathology Services, L V Prasad Eye Institute, Hyderabad 500034, India*

Complete contact information is available at: https://pubs.acs.org/10.1021/acsomega.4c05081

Notes

Financial Disclosure None of the authors have any other financial disclosures.

The authors declare no competing financial interest.

ACKNOWLEDGMENTS

The authors acknowledge the ICMR (No. 5/4/6/17/OPH/2020-NCD-II), the Hyderabad Eye Research Foundation, and

the Hyderabad Lady Tata Memorial Trust Junior Research Fellowship to Agimanailiu Khapuinamai.

REFERENCES

(1) Khan, F. A.; Slain, D.; Khakoo, R. A. Candida endophthalmitis: focus on current and future antifungal treatment options. *Pharmacotherapy* **2007**, *27* (12), 1711−1721.
(2) Gandhi, J.; Sushma, M. V.; Rengan, A. K.; Naik, M. N.; Mishra, D. K.; Boyinpally, S. R.; Joseph, J. Proteomic profiling of exosomes in a mouse model of *Candida albicans* endophthalmitis. *Exp. Cell Res.* **2022**, *417* (2), No. 113222.
(3) Haseeb, A. A.; Elhusseiny, A. M.; Siddiqui, M. Z.; Ahmad, K. T.; Sallam, A. B. Fungal Endophthalmitis: A Comprehensive Review. *J. Fungi* **2021**, *7* (11), No. 996.
(4) Gandhi, J.; Joseph, J. Differential inflammatory response to Aspergillus flavus and *Candida albicans* infection in human retinal pigment epithelial cells: Role in treatment of endophthalmitis. *J. Mycol. Med.* **2021**, *31* (3), No. 101136.
(5) Chhablani, J. Fungal endophthalmitis. *Expert Rev. Anti-Infect. Ther.* **2011**, *9* (12), 1191−1201.
(6) Vallejo-Garcia, J. L.; Asencio-Duran, M.; Pastora-Salvador, N.; Vinciguerra, P.; Romano, M. R. Role of inflammation in endophthalmitis. *Mediators Inflammation* **2012**, *2012*, No. 196094.
(7) Callegan, M. C.; Gilmore, M. S.; Gregory, M.; Ramadan, R. T.; Wiskur, B. J.; Moyer, A. L.; Hunt, J. J.; Novosad, B. D. Bacterial endophthalmitis: therapeutic challenges and host-pathogen interactions. *Prog. Retinal Eye Res.* **2007**, *26* (2), 189−203.
(8) Relhan, N.; Pathengay, A.; Schwartz, S. G.; Flynn, H. W., Jr. Emerging Worldwide Antimicrobial Resistance, Antibiotic Stewardship and Alternative Intravitreal Agents for the Treatment of Endophthalmitis. *Retina* **2017**, *37* (5), 811−818.
(9) Danielescu, C.; Stanca, H. T.; Iorga, R. E.; Darabus, D. M.; Potop, V. The Diagnosis and Treatment of Fungal Endophthalmitis: An Update. *Diagnostics* **2022**, *12* (3), No. 679.
(10) Majji, A. B.; Jalali, S.; Das, T.; Gopinathan, U. Role of intravitreal dexamethasone in exogenous fungal endophthalmitis. *Eye* **1999**, *13* (Pt5), 660−665.
(11) Smeekens, S. P.; van de Veerdonk, F. L.; Kullberg, B. J.; Netea, M. G. Genetic susceptibility to Candida infections. *EMBO Mol. Med.* **2013**, *5* (6), 805−813.
(12) Roemer, T.; Krysan, D. J. Antifungal drug development: challenges, unmet clinical needs, and new approaches. *Cold Spring Harbor Perspect. Med.* **2014**, *4* (5), No. a019703.
(13) Ademe, M. Immunomodulation for the Treatment of Fungal Infections: Opportunities and Challenges. *Front. Cell. Infect. Microbiol.* **2020**, *10*, No. 469.
(14) Tramsen, L.; Schmidt, S.; Roeger, F.; Schubert, R.; Salzmann-Manrique, E.; Latgé, J. P.; Klingebiel, T.; Lehrnbecher, T. Immunosuppressive compounds exhibit particular effects on functional properties of human anti-Aspergillus Th1 cells. *Infect. Immun.* **2014**, *82* (6), 2649−2656.
(15) Hoy, Z.; Wright, T. W.; Elliott, M.; Malone, J.; Bhagwat, S.; Wang, J.; Gigliotti, F. Combination Immunotherapy with Passive Antibody and Sulfasalazine Accelerates Fungal Clearance and Promotes the Resolution of Pneumocystis-Associated Immunopathogenesis. *Infect. Immun.* **2020**, *88* (2), No. e00640.
(16) Matthews, R. C.; Burnie, J. P.; Howat, D.; Rowland, T.; Walton, F. Autoantibody to heat-shock protein 90 can mediate protection against systemic candidosis. *Immunology* **1991**, *74* (1), 20−24.
(17) Pachl, J.; Svoboda, P.; Jacobs, F.; Vandewoude, K.; van der Hoven, B.; Spronk, P.; Masterson, G.; Malbrain, M.; Aoun, M.; Garbino, J.; et al. A randomized, blinded, multicenter trial of lipid-associated amphotericin B alone versus in combination with an antibody-based inhibitor of heat shock protein 90 in patients with invasive candidiasis. *Clin. Infect. Dis.* **2006**, *42* (10), 1404−1413.
(18) Sionov, E.; Segal, E. Polyene and cytokine treatment of experimental aspergillosis. *FEMS Immunol. Med. Microbiol.* **2003**, *39* (3), 221−227.
(19) Sionov, E.; Mendlovic, S.; Segal, E. Experimental systemic murine aspergillosis: treatment with polyene and caspofungin combination and G-CSF. *J. Antimicrob. Chemother.* **2005**, *56* (3), 594−597.
(20) Malek, T. R.; Ortega, G.; Chan, C.; Kroczek, R. A.; Shevach, E. M. Role of Ly-6 in lymphocyte activation. II. Induction of T cell activation by monoclonal anti-Ly-6 antibodies. *J. Exp. Med.* **1986**, *164* (3), 709−722.
(21) Zhang, Z. X.; Stanford, W. L.; Zhang, L. Ly-6A is critical for the function of double negative regulatory T cells. *Eur. J. Immunol.* **2002**, *32* (6), 1584−1592.
(22) Ramadan, R. T.; Ramirez, R.; Novosad, B. D.; Callegan, M. C. Acute inflammation and loss of retinal architecture and function during experimental Bacillus endophthalmitis. *Curr. Eye Res.* **2006**, *31* (11), 955−965.
(23) Khambati, A.; Wright, R. E., III; Das, S.; Pasula, S.; Sepulveda, A.; Hernandez, F.; Kanwar, M.; Chandrasekar, P.; Kumar, A. Aspergillus Endophthalmitis: Epidemiology, Pathobiology, and Current Treatments. *J. Fungi* **2022**, *8* (7), No. 656.
(24) Guest, J. M.; Singh, P. K.; Revankar, S. G.; Chandrasekar, P. H.; Kumar, A. Isavuconazole for Treatment of Experimental Fungal Endophthalmitis Caused by Aspergillus fumigatus. *Antimicrob. Agents Chemother.* **2018**, *62* (11), e01537−18.
(25) Rottmann, B. G.; Singh, P. K.; Singh, S.; Revankar, S. G.; Chandrasekar, P. H.; Kumar, A. Evaluation of Susceptibility and Innate Immune Response in C57BL/6 and BALB/c Mice During *Candida albicans* Endophthalmitis. *Invest. Ophthalmol. Visual Sci.* **2020**, *61* (11), No. 31.
(26) Tang, J.; Lin, G.; Langdon, W. Y.; Tao, L.; Zhang, J. Regulation of C-Type Lectin Receptor-Mediated Antifungal Immunity. *Front. Immunol.* **2018**, *9*, No. 123.
(27) Arce, I.; Martínez-Muñoz, L.; Roda-Navarro, P.; Fernández-Ruiz, E. The human C-type lectin CLECSF8 is a novel monocyte/macrophage endocytic receptor. *Eur. J. Immunol.* **2004**, *34* (1), 210−220.
(28) Zhu, L. L.; Zhao, X. Q.; Jiang, C.; You, Y.; Chen, X. P.; Jiang, Y. Y.; Jia, X. M.; Lin, X. C-type lectin receptors Dectin-3 and Dectin-2 form a heterodimeric pattern-recognition receptor for host defense against fungal infection. *Immunity* **2013**, *39* (2), 324−334.
(29) Tsankov, B. K.; Luchak, A.; Carr, C.; Philpott, D. J. The effects of NOD-like receptors on adaptive immune responses. *Biomed. J.* **2024**, *47* (1), No. 100637.
(30) Katagiri, K.; Hattori, M.; Minato, N.; Kinashi, T. Rap1 functions as a key regulator of T-cell and antigen-presenting cell interactions and modulates T-cell responses. *Mol. Cell. Biol.* **2002**, *22* (4), 1001−1015.
(31) Liu, C.; Whitener, R. L.; Lin, A.; Xu, Y.; Chen, J.; Savinov, A.; Leiding, J. W.; Wallet, M. A.; Mathews, C. E. Neutrophil Cytosolic Factor 1 in Dendritic Cells Promotes Autoreactive CD8+ T Cell Activation via Cross-Presentation in Type 1 Diabetes. *Front. Immunol.* **2019**, *10*, No. 952.
(32) Yang, W. C.; Ghiotto, M.; Barbarat, B.; Olive, D. The role of Tec protein-tyrosine kinase in T cell signaling. *J. Biol. Chem.* **1999**, *274* (2), 607−617.
(33) Isakov, N.; Biesinger, B. Lck protein tyrosine kinase is a key regulator of T-cell activation and a target for signal intervention by Herpesvirus saimiri and other viral gene products. *Eur. J. Biochem.* **2000**, *267* (12), 3413−3421.
(34) Morikawa, Y.; Murakami, M.; Kondo, H.; Nemoto, N.; Iwabuchi, K.; Eshima, K. Natural Killer Cell Group 7 Sequence in Cytotoxic Cells Optimizes Exocytosis of Lytic Granules Essential for the Perforin-Dependent, but Not Fas Ligand-Dependent, Cytolytic Pathway. *Immunohorizons* **2021**, *5* (4), 234−245.
(35) O'Connell, P.; Hyslop, S.; Blake, M. K.; Godbehere, S.; Amalfitano, A.; Aldhamen, Y. A. SLAMF7 Signaling Reprograms T Cells toward Exhaustion in the Tumor Microenvironment. *J. Immunol.* **2021**, *206* (1), 193−205.
(36) Balagopalan, L.; Kortum, R. L.; Coussens, N. P.; Barr, V. A.; Samelson, L. E. The linker for activation of T cells (LAT) signaling

https://doi.org/10.1021/acsomega.4c05081
ACS Omega 2024, 9, 41491−41503

hub: from signaling complexes to microclusters. *J. Biol. Chem.* **2015**, *290* (44), 26422−26429.
(37) Wange, R. L. LAT, the linker for activation of T cells: a bridge between T cell-specific and general signaling pathways. *Sci. STKE* **2000**, *2000* (63), No. re1.
(38) Wang, X.; Yi, P.; Liang, Y. The Role of IL-36 in Infectious Diseases: Potential Target for COVID-19? *Front. Immunol.* **2021**, *12*, No. 662266.
(39) Mabrouk, N.; Tran, T.; Sam, I.; Pourmir, I.; Gruel, N.; Granier, C.; Pineau, J.; Gey, A.; Kobold, S.; Fabre, E.; Tartour, E. CXCR6 expressing T cells: Functions and role in the control of tumors. *Front. Immunol.* **2022**, *13*, No. 1022136.
(40) Kamli, M. R.; Sabir, J. S. M.; Malik, M. A.; Ahmad, A. Human β defensins-1, an antimicrobial peptide, kills Candida glabrata by generating oxidative stress and arresting the cell cycle in G0/G1 phase. *Biomed. Pharmacother.* **2022**, *154*, No. 113569.
(41) Sharma, J.; Mudalagiriyappa, S.; Nanjappa, S. G. T cell responses to control fungal infection in an immunological memory lens. *Front. Immunol.* **2022**, *13*, No. 905867.
(42) Kaur, G.; Singh, N. K. Inflammation and retinal degenerative diseases. *Neural Regener. Res.* **2023**, *18* (3), 513−518.
(43) Riese, M. J.; Moon, E. K.; Johnson, B. D.; Albelda, S. M. Diacylglycerol Kinases (DGKs): Novel Targets for Improving T Cell Activity in Cancer. *Front. Cell Dev. Biol.* **2016**, *4*, No. 108.
(44) Schmidt, S.; Hogardt, M.; Demir, A.; Röger, F.; Lehrnbecher, T. Immunosuppressive Compounds Affect the Fungal Growth and Viability of Defined Aspergillus Species. *Pathogens* **2019**, *8* (4), No. 273.
(45) Rudraprasad, D.; Gandhi, J.; Naik, P.; Naik, M. N.; Naidu, C.; Kumar Mishra, D.; Joseph, J. A Novel and Low-cost Approach for Intravitreal Injection in an Experimental Model of Endophthalmitis. *J. Ophthalmic Vision Res.* **2023**, *18* (3), 272−282.
(46) Naik, P.; Pandey, S.; Naik, M. N.; Mishra, D. K.; Boyenpally, S. R.; Joseph, J. Transcriptomic and Histological Analysis of Exacerbated Immune Response in Multidrug-Resistant Pseudomonas aeruginosa in a Murine Model of Endophthalmitis. *Front. Immunol.* **2022**, *12*, No. 789023.

https://doi.org/10.1021/acsomega.4c05081
ACS Omega 2024, 9, 41491−41503